

PREDICTING STRESS DISTRIBUTIONS EXERTED ON LCM TOOLS DURING FILLING PHASES

W. A. Walbran¹, S. Bickerton^{1,3}, P. A. Kelly²

Centre for Advanced Composite Materials,

¹*Department of Mechanical Engineering,*

²*Department of Engineering Science,*

The University of Auckland, Private Bag 92019, Auckland 1020, New Zealand

³*Corresponding author: s.bickerton@auckland.ac.nz*

SUMMARY: Mould tools used for LCM processes such as Resin Transfer Moulding (RTM) and Injection/Compression Moulding (I/CM) must withstand local forces due to resin pressure and compaction of the fibre reinforcement. Prediction of these tooling forces will allow cost effective mould design and process selection. A series of RTM and I/CM experiments have been undertaken, monitoring total clamping force and normal stress distribution acting on mould surfaces. A mixed elastic and a visco-elastic reinforcement compaction model have been used to model these processes, both being compared to experimental data. Both models show good agreement to experiment during compaction phases, however the visco-elastic model matches the experimental data significantly better during periods influenced by stress relaxation. Circumferentially averaged stress distributions are also compared at key points in the process, both models showing good qualitative agreement to experiment, and the RTM cases also matching well quantitatively. Overall, the RTM process has been modeled accurately, while some discrepancy exists for I/CM during secondary compaction, when fluid is compressed along with reinforcement.

INTRODUCTION

The term Liquid Composite Moulding (LCM) encompasses processes such as Resin Transfer Moulding (RTM), Injection/Compression Moulding (I/CM), and Resin Infusion (a.k.a. VARTM). To date, various simulations have been employed to model the filling phase of these processes [1-3] and recently these have been extended to cover the total forces experienced by the mould tools [4,5]. Accurate tooling force predictions for LCM processes will allow reductions in setup time and cost by allowing for appropriate mould tool design, and appropriate selection of supporting equipment. This paper presents a series of RTM and I/CM experiments. These results are compared to simulations using different reinforcement compaction models. Total clamping force and normal stress distributions exerted on a mould have been measured and recorded. The

TekScan distributed pressure monitoring system has been used to measure normal stress distributions during entire experimental cycles.

RTM can be divided into four separate phases; preform preparation, mould closure, resin injection and finally cure. A fibre preform is inserted into a mould, which is then closed to a set cavity thickness, determining the fibre volume fraction (V_f) of the final part. A thermoset resin is then injected into the mould until complete wet-out of the preform is achieved and the injection gate(s) closed. The resin is then cured before the finished part is removed.

I/CM is similar to RTM, but with an additional compaction phase, resulting in a five-phase process; preform preparation, mould closure to initial cavity thickness, injection of resin, mould closure to final cavity thickness and finally resin cure. The mould is closed to an initial cavity thickness greater than that of the desired final part thickness, and a measured volume of resin is injected. With the full volume of resin injected, the injection gate(s) are closed and the mould is closed to the desired final cavity thickness (and hence V_f). This provides compression driven flow to complete wet-out of the preform, potentially providing significantly faster cycle times than those achievable with a comparable RTM process [6].

NUMERICAL

Common practice for modeling flow through reinforcements is to use Darcy's law [1-4]. A one-dimensional consolidation approach is used here to relate total normal stress experienced by the laminate (σ_{TOT}) to local fluid pressure (P) and fibre compaction stress (σ) [4];

$$\sigma_{TOT} = \sigma + P. \quad (1)$$

Two reinforcement compaction models are applied in this study, a mixed-elastic and a visco-elastic model. The visco-elastic model used here incorporates two separate models, accounting for compaction and relaxation separately, the mixed-elastic using the compaction model only, assuming that all stress relaxation occurs instantaneously to the long term stress.

Compaction Response

Previous studies have shown that compaction response of reinforcements varies with V_f and compaction speed \dot{h} [7]. Compaction curves can be normalised, time with respect to the time taken to reach the final V_f , and stress with respect to stress at the final V_f . When applied to Chopped Strand Mat (CSM), these normalised curves collapse onto a single master curve. A compaction model for materials which respond in this way was developed and described in [8]. The principal features of this model are briefly described below.

This ‘‘collapsing curves’’ response mentioned above implies that the stress, a function of V_f and \dot{h} , decomposes multiplicatively according to;

$$\sigma(V_f, v) = f_\alpha(v) f_\beta(V_f). \quad (2)$$

One method of deriving expressions for the functions f_α, f_β , is to examine compaction curves at a reference V_f and a reference compaction speed. The choice of references which are typical for the process under study are preferable, but not critical. Let $\sigma_\beta(V_f)$ be the stress (compaction curve) corresponding to the reference compaction speed v^{ref} ; it is a smooth monotonic curve and can be represented accurately using a simple polynomial function;

$$\sigma_\beta(V_f) = \sum_{i=0}^{N_\beta} \beta_i (V_f - V_f^{dat})^i, \quad (3)$$

where V_f^{dat} is some chosen (small) datum volume fraction corresponding to a measured nominal stress. Determination of σ_β requires only a single experiment. A second function, $\sigma_\alpha(v)$, is the stress at the reference volume fraction V_f^{ref} . Due to the rapid initial increase in stress with compaction speed, a polynomial fit is inadequate. One possibility is to model this behaviour using a function of the form

$$\sigma_\alpha(v) = \sigma_\alpha(\infty) - (\sigma_\alpha(\infty) - \sigma_\alpha(0)) \frac{1}{N} \sum_{i=1}^{N_\alpha} e^{-\alpha_i \left(\frac{v}{v^{ref}}\right)} \quad (4)$$

where $\sigma_\alpha(\infty)$ and $\sigma_\alpha(0)$ are the stresses at ‘very fast’ and ‘very slow’ speeds, at V_f^{ref} , respectively. This expression can be adequately determined from four compaction tests, carried out at different speeds. Let $\lambda = \sigma_\alpha(v^{ref}) = \sigma_\beta(V_f^{ref})$, the stress at any given V_f and \dot{h} can then be determined from

$$\sigma(V_f, v) = \frac{1}{\lambda} [\sigma_\alpha(v) \sigma_\beta(V_f)] \quad (5)$$

Stress Relaxation Response

A few models have been proposed which incorporate the viscoelastic response of fibrous materials, e.g. [7,9]. A viscoelastic model which incorporates the ‘‘collapsing curve’’ response has also been presented in [8]. The stress can be expressed as a summation of $\sigma_{eq}(V_f)$, the equilibrium stress, i.e. the stress at infinitely slow compaction velocity, and q , the viscous stress. In general, q can be determined by solving a differential equation [7]. However, at constant V_f , the differential equation can be solved exactly;

$$q(t) = [At^n + q_0^{-m}]^{\frac{1}{m}}, \quad (6)$$

where $m = (n-1)/n$, $A = nE^{1/n}/\eta$, q_0 is the viscous stress at the start of relaxation, and n , E and η are material parameters [7,8]. Incorporating the collapsing behaviour gives:

$$\sigma(\bar{t}) = \frac{\sigma^R}{\sigma_\beta(V_f)} \left[\sigma_{eq}(V_f) + \left(A \left(\bar{t} \frac{v}{v^{ref}} \right)^n + (\sigma_\beta(V_f) - \sigma_{eq}(V_f))^{-m} \right)^{\frac{1}{m}} \right], \quad (7)$$

where \bar{t} is the time since the onset of relaxation, σ^R is the stress at the onset of relaxation, v the compaction speed prior to relaxation, $\sigma_{eq}(V_f)$ can be determined using Eqn. 5 and the three relaxation parameters are A , m and n . This approach models the collapsing of relaxation curves at a certain V_f . As the relaxation behaviour also depends on V_f one of the parameters must vary with V_f . In this case it is assumed to be A , which can be expressed as a polynomial;

$$A(V_f) = \sum_{i=0}^{N_A} A_i V_f^i. \quad (8)$$

Table 1 presents the model parameters for CSM, as determined in this study.

Table 1 Model parameters for CSM

$v^{ref} = 2\text{mm/min}, V_f^{ref} = 0.425, N_\alpha = 4, N_\beta = 4, N_A = 2, V_f^{dat} = 0.425$											
DRY CSM			WET CSM								
α_1	8000	β_0	76129	A	-0.0233	α_1	80	β_0	79721	A_0	0.0421
α_2	2.9	β_1	1193200	A	0.0197	α_2	1.5	β_1	1249100	A_1	-0.0428
α_3	0.8	β_2	7890000	A	-0.0036	α_3	1.23	β_2	7786100	A_2	0.0111
α_4	0.85	β_3	2825300	m	0.5000	α_4	1.25	β_3	2395900	m	0.5495
$\sigma_\alpha(\infty)$	90000	β_4	4702700	n	0.5000	$\sigma_\alpha(\infty)$	30000	β_4	30040000	n	0.5331
$\sigma_\alpha(0)$	30000					$\sigma_\alpha(0)$	94000				

EXPERIMENTAL SETUP AND PROGRAM

Shown in Fig. 1 is a schematic of the experimental facility used for this study. The mould is mounted in an Instron 1186 universal testing machine which provides accurate displacement and velocity control. A spherical crosshead mount allows accurate parallel alignment of the platens, providing consistent V_f across the part.

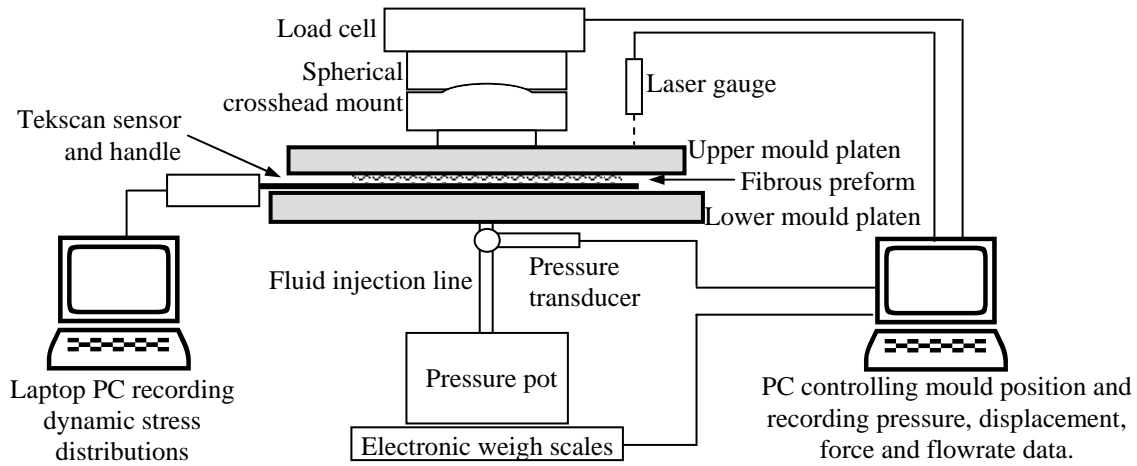


Fig. 1 Schematic of experimental setup.

Test fluid was injected via a pressure pot, pressure being maintained constant within courtesy of an electronic regulator. The injection pressure was measured using a transducer. The mass of

fluid injected was monitored continuously in all cases using electronic weigh scales. A laser gauge was used to measure the cavity thickness when under load. Injection pressure, mass of fluid, cavity thickness and applied load were all recorded using the Instron's Bluehill software. The Tekscan system provides dynamic measurement of pressure distribution at rates up to 8.0 Hz. This study utilised 238 mm square sensors having a grid of 44 by 44 sensels. Two sensors were used, with pressure ranges of 0-200 kPa and 0-1303 kPa.

Procedure

RTM preforms were laid up inside the mould and the mould closed, at a constant rate (\dot{h}_1). When the target V_f was achieved, the cavity thickness (h_2) was held constant by the Instron while fluid was injected at constant pressure. Once the measured volume of fluid had been injected, the injection gate was closed. The I/CM process differs from the RTM process, in that the fluid was injected at a cavity thickness (h_1) greater than the final cavity thickness, and a measured volume of fluid injected. The injection gate was then closed, and the mould closed to the target V_f at a constant rate (\dot{h}_2).

To achieve a wide range of situations for comparison to simulation, a number of experimental parameters were varied. A subset of these experiments is presented in Table 2. The final cavity thickness in all cases was 3.5mm, different V_f 's achieved by altering the number of layers of reinforcement in each preform (10 layers for $V_f = 0.50$ and 7 layers for $V_f = 0.35$). Preforms were cut to a diameter of 200mm, with a central 15mm diameter hole punched to enforce two-dimensional fluid flow. In this study, 450g/m² CSM reinforcement has been used. The test fluid in all cases was Mobil DTE AA mineral oil (viscosity 1.16 Pa.s at 20°C).

Table 2 Experimental parameters

	V_f	h_1 (mm)	\dot{h}_2 (mm/min)	P_{inj} (kPa) nominal	P_{inj} (kPa) measured
RTM2	0.35	-	-	400	405
RTM4	0.50	-	-	400	445
I/CM4	0.35	4.1	10	400	363
I/CM8	0.50	4.4	10	400	415

EXPERIMENTAL RESULTS AND DISCUSSION

Presented in Fig. 2 are stress distributions during both RTM experiments at major stages of the process. These plots highlight significant local stress fluctuations, despite the relatively homogeneous physical appearance of CSM. This is especially apparent at the high V_f . It is clear that the total stress at the end of filling for low V_f (Fig. 2b) is significantly influenced by the fluid pressure. This is expected, as only moderate force is required to compress the preform to the desired V_f (0.35). Conversely, much higher forces are required to compress the preform to the high V_f (0.50), so fluid pressure plays a less significant role (Fig. 2e). The influence of stress relaxation is clearly demonstrated when comparing normal stress levels at the end of compaction (Fig. 2a and 2d), with the long term stress state (Fig. 2c and 2e).

a)

b)

c)

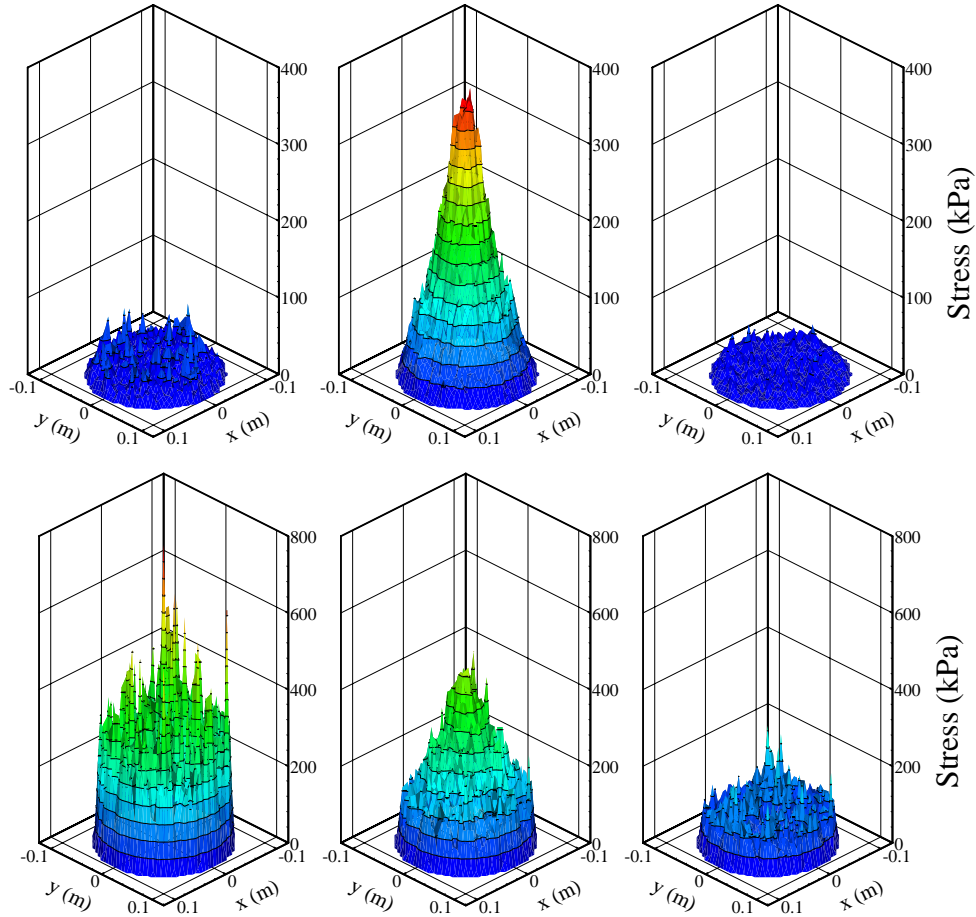


Fig. 2 Stress distributions during RTM: a) RTM2; d) RTM4 the end of compaction; b) RTM2; e) RTM4 end of filling; c) RTM2; f) RTM4 long term relaxed states.

Fig. 3 presents similar distributions during the I/CM experiments. As with RTM, in the low V_f case fluid pressure is more prominent than compaction stress. At the completion of the injection stage (Fig. 3b), fluid pressure dominates the compaction stress. After secondary compression (Fig. 3c) compaction stress has increased, however total stress is still dominated by fluid pressure. For the high V_f case, the higher fibre compaction stress is more prominent, particularly at the end of secondary compaction. However, the majority of the total stress is still due to fluid pressure at the completion of the compression flow phase. This observation is confirmed by the large drop in total force at the completion of filling (Fig. 5).

Comparison to Simulation

Fig. 4 presents total clamping force traces for both RTM cases, comparing the experiment to predictions made using both compaction models. For low V_f , maximum clamping force is experienced at the end of injection, whereas for high V_f it is at the end of compaction. This reinforces observations of the normal stresses (Fig. 3). In both cases predicted forces show good agreement with experiment. Fill times are slightly over predicted (13% and 8% for low and high V_f respectively). During filling, when stress relaxation is occurring, the visco-elastic model provides a closer fit to the experimental data. This is due to the nature of the mixed-elastic model,

which assumes all relaxation occurs instantaneously. The predicted drop at the end of injection is similar to experiment, indicating that fluid force is modeled accurately.

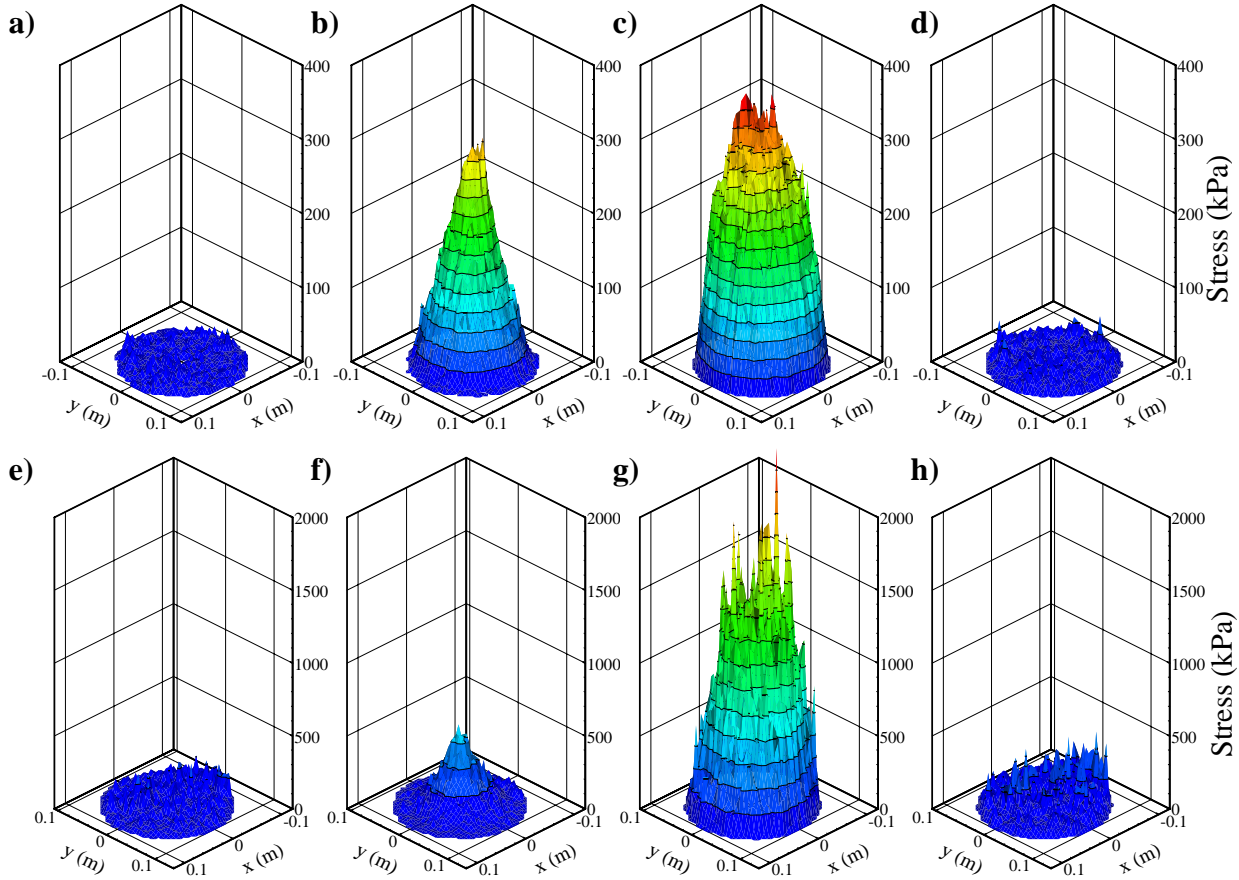


Fig. 3 Normal stress distributions during I/CM at $V_f = 0.50$ and $P_{Inj,Pot} = 400$ kPa: a) I/CM4; e) I/CM8 the end of primary compaction; b) I/CM4; f) I/CM8 end of filling; c) I/CM4; g) I/CM8 end of secondary compaction; d) I/CM4; h) I/CM8 long term relaxed states.

Fig. 5 presents force traces for both I/CM cases. As with RTM, during initial filling both models show good agreement with experiment. The time to completion of filling is well predicted for the high V_f , but less so for the low V_f case. During secondary compaction, both models over predict the total clamping force, particularly for high V_f . Comparison of the predicted and recorded gate pressures during this period shows that fluid pressure is over predicted to a similar degree. Assuming that the experimental compression phase was carried out correctly, this over prediction of fluid pressure and force during secondary compaction could point to a compression history dependence for permeability. This has been observed previously [4]. After secondary compaction, the visco-elastic model is providing very good agreement with experiment, especially at the high V_f , while the mixed-elastic model displays some difference during this fibre relaxation phase.

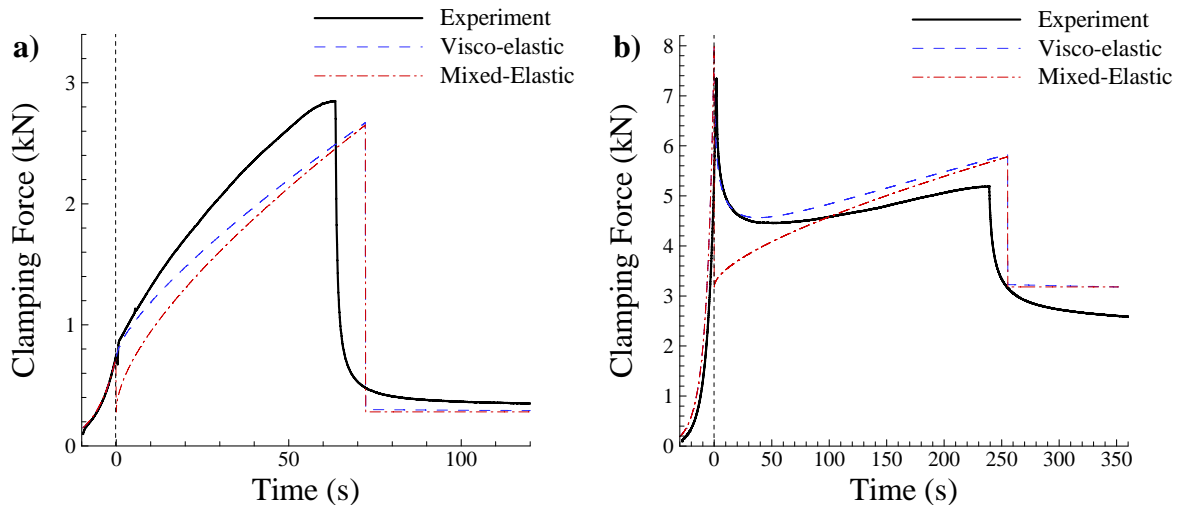


Fig. 4 Force traces for RTM: a) $V_f=0.35$ and b) $V_f=0.50$.

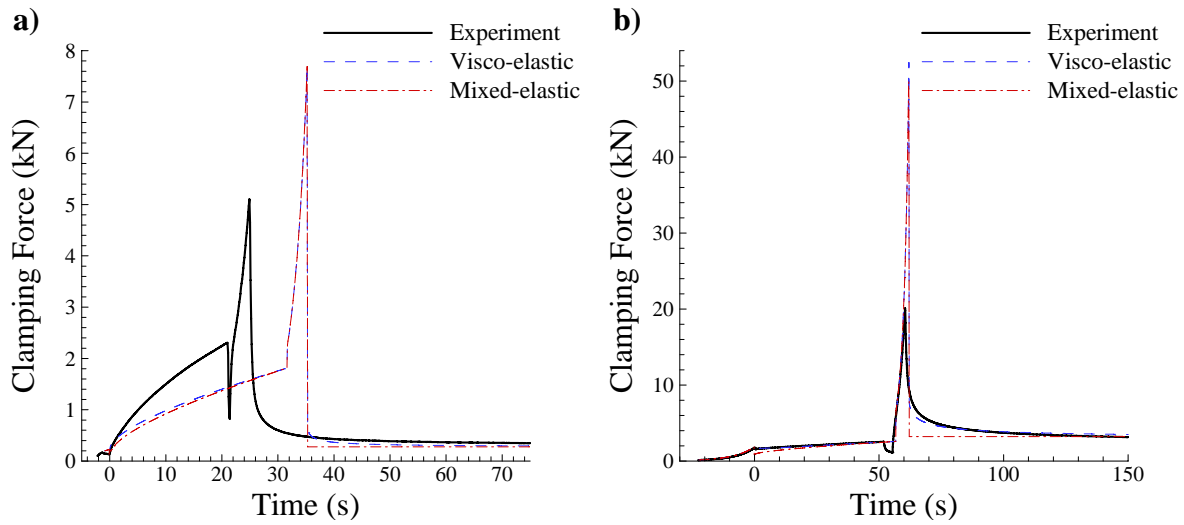


Fig. 5 Force traces for I/CM: a) $V_f=0.35$ and b) $V_f=0.50$.

While not as significant for these cases, the improved accuracy of the visco-elastic model during relaxation may have significant benefits when modeling force-controlled processes. Shown in Fig. 6 are circumferentially averaged normal stresses experienced by the mould plotted against radius during RTM, at two points in the process, when the flow front (r_f) reaches 0.05 m, and at the completion of filling. Predicted normal stress data is also presented.

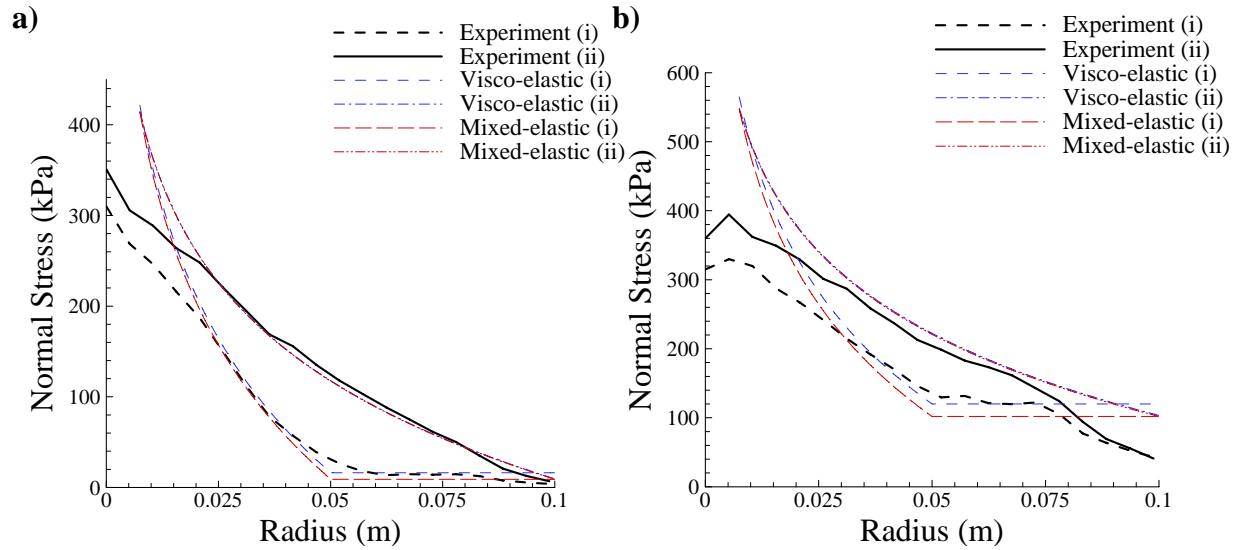


Fig. 6 Averaged radial normal stresses experienced by the mould during RTM: a) $V_f = 0.35$; and b) $V_f = 0.50$ at i) $r_f = 0.05$ m, and ii) end of filling.

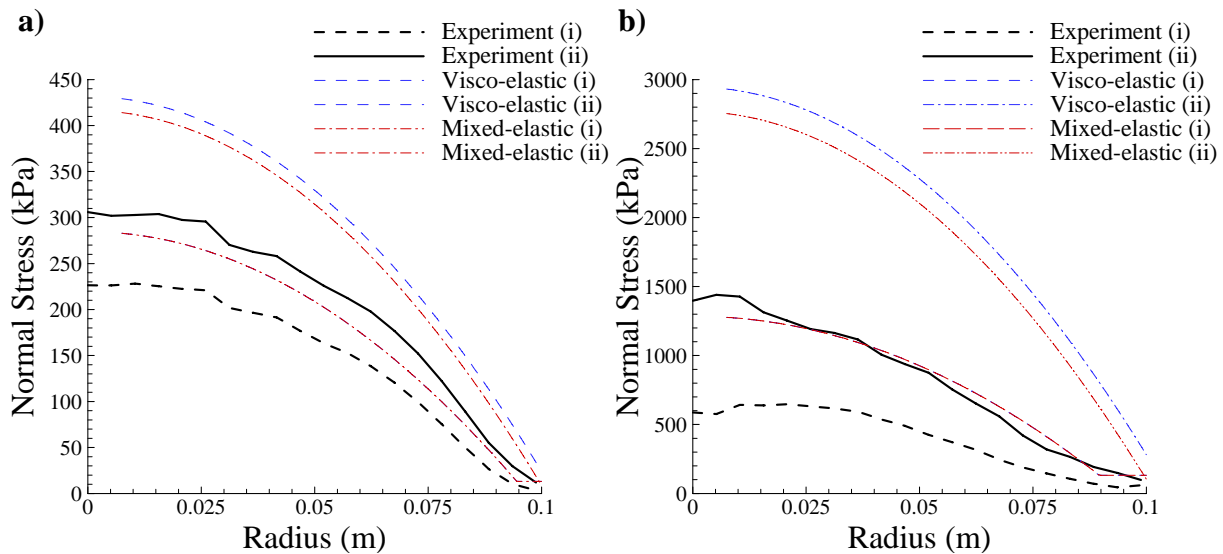


Fig. 7 Averaged radial normal stresses experienced by the mould during RTM: a) $V_f = 0.35$; and b) $V_f = 0.50$ at i) half way through secondary compaction phase, and ii) end of filling.

For both values of V_f , the stress at the inlet is over predicted at both time instances. At $r_f = 0.05$ m, for both values of V_f the visco-elastic model provides a very good fit to the experimental data from approximately $r = 0.02$ m. At the end of filling, the majority of stress relaxation has taken place, both models predicting the same stress distribution. At this point, both models are showing good agreement from $r = 0.02$ m, the high V_f over predicting slightly, reinforcing observations made from Fig. 4. In all cases, there is a drop in observed stress at the outer edge of the preform (approaching $r = 0.1$ m). This could be attributed to irregularities in the unconstrained edge of the preform, reducing compaction stress in this region.

Fig. 7 presents similar distributions for I/CM, half way through, and at the completion of the secondary compaction phase. In both cases, the predicted distributions are showing good qualitative agreement with experiment. The predicted pressure levels are significantly greater than for the experiments, confirming observations on the total clamping force (Fig. 5). For both values of V_f , the stress predicted by both models is identical, as during this phase the reinforcement is being compacted.

CONCLUSIONS

Mould tools used for LCM processes such as RTM and I/CM must withstand the forces generated by the fluid and reinforcement within. A series of LCM experiments has been undertaken, a subset of which is presented here. Observations of normal stress acting on mould tools have been made using the Tekscan dynamic pressure monitoring system. Tekscan has highlighted the local stress variation during compaction of CSM, as well as reinforcing previous observations regarding stress relaxation of reinforcements. Two reinforcement compaction models have been utilized in modeling the LCM processes: a mixed-elastic and a visco-elastic model. Both have shown good agreement with experimental data during compaction phases, the visco-elastic model providing greater accuracy when thickness is held constant.

REFERENCES

1. A. Shojaei, "A Numerical Study of Filling Process Through Multilayer Preforms in Resin Injection/Compression Molding", *Composites Science and Technology*, Vol. 66, no.'s 11-12, 2006, pp. 1546-1557.
2. P. Simacek, and S. G. Advani, "Desirable Features in Mold Filling Simulations for Liquid Composite Molding Processes", *Polymer Composites*, Vol. 25, no. 4, 2004, pp. 355-367.
3. F. Trochu, Edu Ruiz, V. Achim and S. Soukane, "Advanced Numerical Simulation of Liquid Composite Molding for Process Analysis and Optimization", *Composites Part A: Applied Science and Manufacturing*, Vol. 37, no. 6, 2006, pp 890-902.
4. S. Bickerton, and M. J. Buntain, "Modeling Forces Generated Within Rigid Liquid Composite Molding Tools. Part B: Numerical Analysis", *Composites Part A: Applied Science and Manufacturing*, Vol. 38, no. 7, 2007, pp.1742-1754.
5. S. Bickerton, and P. A. Kelly, "Application of a Complete Tooling Force Analysis for Simulation of Liquid Composite Moulding Processes", *Key Engineering Materials*, Vol. 334-335 I, 2007, pp.17-20.
6. S. Bickerton, and M. Z. Abdullah "Modeling and Evaluation of the Filling Stage of Injection/Compression Moulding", *Composites Science and Technology* Vol. 63, no. 10, 2003, pp. 1359-1375.
7. P. A. Kelly, R. Umer, S. and Bickerton, "Viscoelastic Response of Dry and Wet Fibrous Materials during Infusion Processes", *Composites Part A: Applied Science and Manufacturing*, Vol. 37, no.6, 2006, pp. 868-873.
8. P. A. Kelly, "A Fibre Compaction Model for Liquid Composite Moulding", *The 6th Canadian Int. Composites Conference (CANCOM 2007)*, Winnipeg, Canada, 14th-17th August, 2007.
9. J. Breard, Y. Henzel, F. Trochu, and R., Gauvin, "Analysis of Dynamic Flows Through Porous Media Part II: Deformation of a Double-Scale Fibrous Reinforcement". *Polymer Composites*, Vol. 24, no.3, 2003, pp. 409-421.